

6-1-1998

Nanostructured NdFeB films processed by rapid thermal annealing

M. Yu

University of Nebraska - Lincoln

Yi Liu

University of Nebraska - Lincoln, yliu@unlserve.unl.edu

Sy_Hwang Liou

University of Nebraska-Lincoln, sliou@unl.edu

David J. Sellmyer

University of Nebraska-Lincoln, dsellmyer@unl.edu

Follow this and additional works at: <http://digitalcommons.unl.edu/physicsliou>

 Part of the [Physics Commons](#)

Yu, M.; Liu, Yi; Liou, Sy_Hwang; and Sellmyer, David J., "Nanostructured NdFeB films processed by rapid thermal annealing" (1998).
Si-Hwang Liou Publications. Paper 70.
<http://digitalcommons.unl.edu/physicsliou/70>

This Article is brought to you for free and open access by the Research Papers in Physics and Astronomy at DigitalCommons@University of Nebraska - Lincoln. It has been accepted for inclusion in Si-Hwang Liou Publications by an authorized administrator of DigitalCommons@University of Nebraska - Lincoln.

Nanostructured NdFeB films processed by rapid thermal annealing

M. Yu,^{a),b)} Y. Liu,^{c)} S. H. Liou,^{a)} and D. J. Sellmyer^{a)}

Center for Materials Research and Analysis, University of Nebraska, Lincoln, Nebraska 68588-0113

Nanostructured NdFeB films were prepared by magnetron sputtering followed by rapid thermal annealing at a ramp rate of 200 °C/s. Isotropically oriented Nd₂Fe₁₄B crystallites were formed in the films and coercivities up to 20 kOe and remanence ratios up to 0.8 were obtained. Transmission electron microscopy analysis shows that the majority phase of the magnetic layer in the high coercivity films consists of Nd₂Fe₁₄B nanocrystallites with an average size of about 50 nm. These nanocrystallites are believed to be single-domain particles, which are responsible for the high coercivities. MFM measurements show that the domain size is about 500 nm. It is thus indicated that the 50 nm Nd₂Fe₁₄B nanocrystallites are strongly exchange-coupled into the 500 nm domains and the high remanence ratio originates from this exchange coupling. © 1998 American Institute of Physics. [S0021-8979(98)44111-2]

I. INTRODUCTION

Since the discovery of Nd₂Fe₁₄B in 1984,¹⁻³ numerous studies on NdFeB-based materials have been conducted to obtain a better understanding of their excellent intrinsic properties and develop better fabrication processes for permanent magnets.⁴ Most of this research was on bulk NdFeB materials and relatively only a little work has been done on thin film NdFeB materials.⁵⁻¹³ With the rapid development of micromechanical devices, microelectronics, and integrated magneto-electronic devices, applications of permanent magnet films are becoming more significant. Furthermore, better knowledge of NdFeB films also can help one to understand the exchange coupling in nanostructured magnetic materials because films thickness and grain sizes can be controlled to some extent to test some recent theoretical calculations.^{14,15}

In this article we report our systematic study of the magnetic properties of nanostructured NdFeB films prepared from amorphous state by rapid thermal annealing (RTA). RTA features a very high ramp rate (200 °C/s) and thus is able to anneal films for a very short effective annealing time (tens of seconds), which is essential in forming isotropic nanostructured NdFeB films with high coercivities (H_c) and high remanence ratios (M_r/M_s).

II. EXPERIMENTAL METHODS

All NdFeB films were deposited directly onto water-cooled 7059 glass substrates at room temperature by dc magnetron sputtering with base pressure of better than 3×10^{-7} Torr and Ar pressure of 10 mTorr. The NdFeB layer has a thickness of 500 nm and is protected by a 40 nm Cr overcoat. The Nd₁₅Fe₇₇B₈ target was provided by Electron Energy Company and some Nd chips were added to adjust the Nd concentration. The composition of the films is Nd₃₀Fe₆₃B₇, which was estimated by the area ratio of Nd chips and the target and verified by energy-dispersive x-ray measurements. The as-deposited films were all processed by

RTA technique (unless specified otherwise) in flowing Ar with a ramp rate of 200 °C/s. The structure and microstructure were characterized by x-ray diffraction (XRD) and transmission electron microscopy (TEM) measurements. The magnetic properties at room temperature were determined by a SQUID magnetometer and the magnetic domain size was estimated by MFM measurements.

III. RESULTS AND DISCUSSION

The XRD pattern of an as-deposited NdFeB film is shown in Fig. 1. Magnetic measurements showed that the as-deposited films are magnetically soft. It is thus indicated as expected that the as-deposited films are amorphous except for the presence of a little α -Fe. Figure 1 also shows the XRD pattern of the NdFeB film annealed at 500 °C for 60 s. Nd₂Fe₁₄B crystallites were formed and they were found to be isotropically oriented in the annealed film, as indicated by the peaks in Fig. 1. In fact all properly annealed films (i.e.,

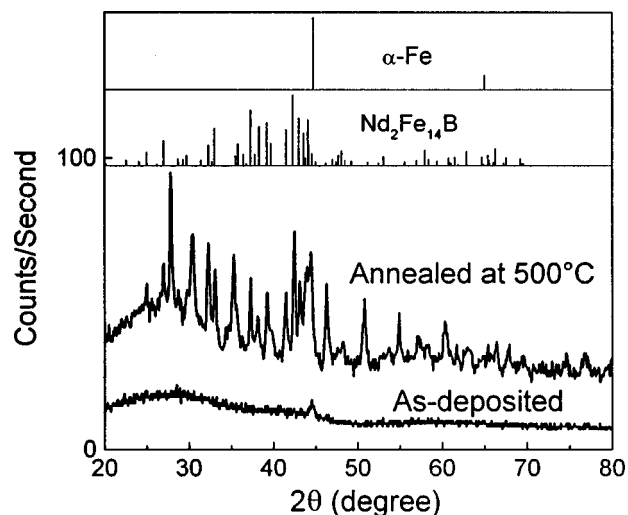


FIG. 1. X-ray diffraction patterns of as-deposited and annealed (500 °C, 60 s) NdFeB films. The standard diffraction patterns of α -Fe and Nd₂Fe₁₄B phases are also shown for comparison.

^{a)}Department of Physics and Astronomy.

^{b)}Electronic mail: myu@unlinfo.unl.edu

^{c)}Department of Mechanical Engineering.

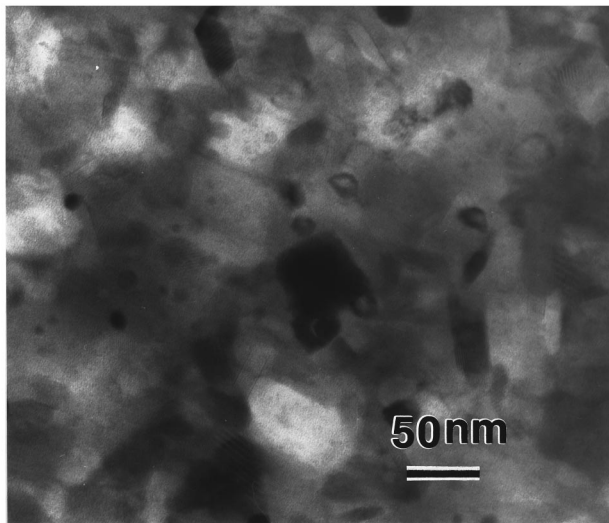


FIG. 2. TEM picture of a NdFeB film annealed at 500 °C for 60 s.

those with $H_c > 5$ kOe) consist of isotropically oriented $\text{Nd}_2\text{Fe}_{14}\text{B}$ crystallites, as confirmed by both XRD and magnetic measurements (see later discussion).

The XRD pattern of the annealed NdFeB film has peaks other than those of $\text{Nd}_2\text{Fe}_{14}\text{B}$. They can all be indexed to Nd_2O_3 and NdO phases. The oxygen was mainly introduced in the RTA process which in our case can be done only in flowing Ar.

The formation of the $\text{Nd}_2\text{Fe}_{14}\text{B}$ phase is only one necessary condition to have high H_c and M_r/M_s in NdFeB films. The other is that appropriate microstructure must be developed. Figure 2 is the bright field TEM picture of the NdFeB film annealed at 500 °C for 60 s. Electron diffraction analysis indicates that the grains shown in Fig. 2 are $\text{Nd}_2\text{Fe}_{14}\text{B}$ crystallites. The size of these crystallites is about 50 nm. This means that these nanocrystallites are single-domain particles because the critical single-domain particle diameter of

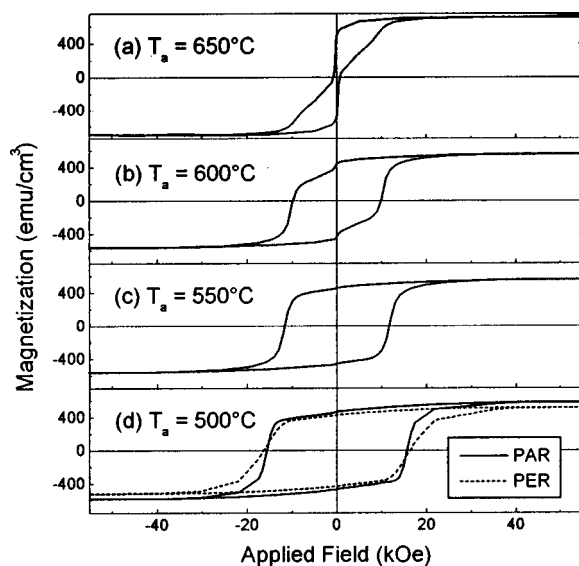


FIG. 3. Hysteresis loops of NdFeB films annealed for 60 s at various temperatures (T_a).

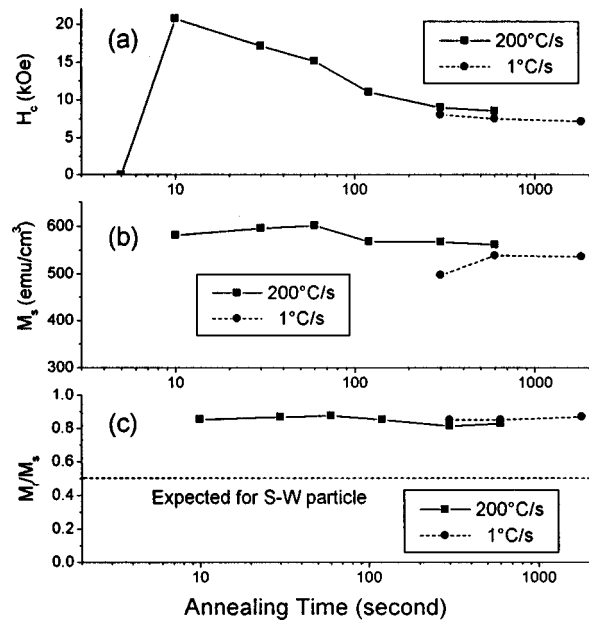


FIG. 4. (a) H_c , (b) M_s , and (c) M_r/M_s of NdFeB films annealed at 550 °C for various times with ramp rates of 200 and 1 °C/s.

$\text{Nd}_2\text{Fe}_{14}\text{B}$ is about 300 nm.⁴ The composition of the film indicates that there should be a thin Nd-rich layer between the nanocrystalline $\text{Nd}_2\text{Fe}_{14}\text{B}$ particles, although it cannot be seen due to limited resolution. The high ramp rate may also introduce some defects other than the Nd-rich layer.

With the change of structure and microstructure in Nd-FeB films, the magnetic properties are also changed completely after annealing. Figure 3(d) shows the parallel and perpendicular hysteresis loops of the NdFeB film annealed at 500 °C for 60 s. The large H_c (~ 16 kOe) and the similarity of the two loops also indicate the formation of isotropically oriented $\text{Nd}_2\text{Fe}_{14}\text{B}$ nanocrystallites in a Nd-Fe-B system. In addition to the formation of the $\text{Nd}_2\text{Fe}_{14}\text{B}$ phase, the microstructure (the 50 nm nanocrystallites and the associated defects) also plays an important role in developing high H_c .

Annealing temperature (T_a) and time (t_a) can strongly affect the magnetic properties. Figure 3 shows the hysteresis loops of the NdFeB films annealed for 60 s at various T_a . We observed that no H_c can be developed if $T_a < 500$ °C. After T_a reaches 500 °C, H_c is developed but decreases and the saturation magnetization M_s changes slightly as T_a increases. If $T_a > 650$ °C, H_c decreases sharply with a moderate increase of M_s . These results have the following implications. First, the crystallization of $\text{Nd}_2\text{Fe}_{14}\text{B}$ can occur only when $T_a \geq 500$ °C, which is less than 627 °C, the crystallization temperature of $\text{Nd}_2\text{Fe}_{14}\text{B}$.⁴ This is reasonable because the crystallization temperature decreases when Nd concentration increases.¹⁶ Second, when $T_a > 500$ °C, presumably the $\text{Nd}_2\text{Fe}_{14}\text{B}$ nanocrystallites grow and the defects are reduced. This is the most probable reason for the decrease of H_c with the increase of T_a . Finally when $T_a \geq 650$ °C, most Nd is oxidized and α -Fe is left as the main magnetic phase, causing the sharp decrease of H_c and the increase of M_s .

Another batch of NdFeB films was annealed at 550 °C for various t_a and the resulting H_c , M_s , and M_r/M_s are

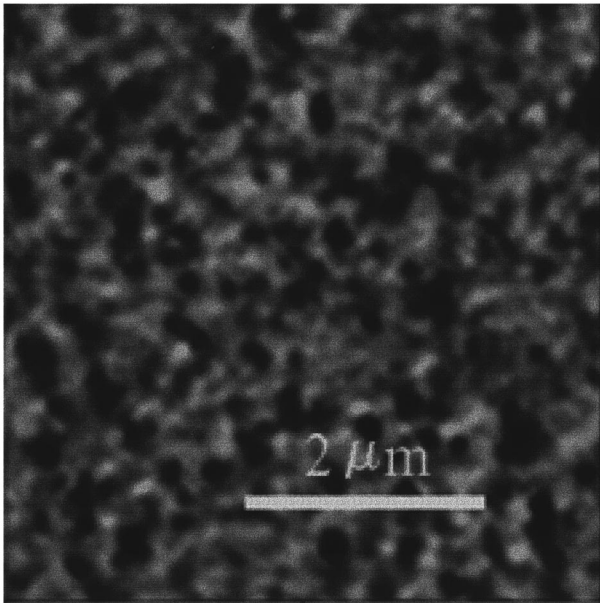


FIG. 5. MFM image of a thermally demagnetized NdFeB film annealed at 500 °C for 60 s. The CoCr MFM tip was magnetized parallel to the sample surface.

plotted in Fig. 4. It is noted that t_a has a strong effect on H_c but a weak one on M_s . Short t_a is critical to obtain high H_c , but $t_a < 10$ s is too short to achieve the proper crystallization of Nd₂Fe₁₄B for high H_c . When $T_a > 500$ °C, longer t_a has essentially the same effect as higher T_a on the microstructure, i.e., the Nd₂Fe₁₄B nanocrystallites grow and the defects are reduced. In turn H_c decreases and M_s changes slightly as t_a increases. The general effects of T_a and t_a on H_c are in agreement with the results obtained in melt-spun NdFeB materials.¹⁶

For comparison we also annealed the as-deposited films at 550 °C in a conventional oven with a ramp rate of 1 °C/s. The resulting H_c , M_s , and M_r/M_s are also shown in Fig. 4. Because of the low ramp rate, the total effective annealing time of the conventional oven is longer than that of RTA for the same t_a . Thus the H_c obtained by the conventional oven is smaller than that obtained by RTA. This result clearly demonstrates the importance of high ramp rate when very short annealing time is needed.

We have shown that the Nd₂Fe₁₄B nanocrystallites are isotropically oriented in the annealed films. According to Stoner–Wohlfarth theory¹⁷ such a system should have a M_r/M_s of 0.5 if there is no interaction among the Nd₂Fe₁₄B nanocrystallites. But Fig. 4(c) shows that these isotropic NdFeB films have $M_r/M_s > 0.8$. The high M_r/M_s must come from the strong exchange coupling among the Nd₂Fe₁₄B nanocrystallites. This phenomenon was observed in melt-spun isotropic NdFeB materials¹⁸ and predicted in theoretical

calculations.¹⁹ A MFM image of a thermally demagnetized NdFeB film annealed at 500 °C for 60 s is shown in Fig. 5. It can be estimated that the domain size is about 500 nm. This means that in one domain there are many Nd₂Fe₁₄B nanocrystallites aligned by exchange coupling. Such a micromagnetic structure (sometimes called “an interaction domain”) provides a direct explanation for the high M_r/M_s . The exchange coupling here is so strong that M_r/M_s is changed slightly when H_c is changed dramatically.

IV. CONCLUSIONS

By using the RTA technique we are able to fabricate isotropic nanocrystalline NdFeB films with high H_c and high M_r/M_s . H_c is very sensitive to annealing temperature and time. Low temperature and short time, which are *just* enough to crystallize the amorphous NdFeB into single-domain Nd₂Fe₁₄B nanocrystallites, are critical to obtain the proper microstructure for high H_c . We also found that these high coercivity, nanocrystalline NdFeB films have very high M_r/M_s , which originates from the strong exchange coupling among the Nd₂Fe₁₄B nanocrystallites.

ACKNOWLEDGMENTS

The authors would like to thank Professor R. D. Kirby and Dr. Z. S. Shan for their generous help. This work was supported by DOE and CMRA. S. H. Liou was also supported by ARO/DAAG55-98-1-0014.

- ¹J. J. Croat, J. F. Herbst, R. W. Lee, and F. E. Pinkerton, J. Appl. Phys. **55**, 2078 (1984).
- ²M. Sagawa, S. Fujimura, M. Togawa, H. Yamamoto, and Y. Matsuura, J. Appl. Phys. **55**, 2083 (1984).
- ³D. J. Sellmyer, A. U. Ahmed, and G. C. Hadjipanayis, J. Appl. Phys. **55**, 2088 (1984).
- ⁴J. F. Herbst, Rev. Mod. Phys. **63**, 819 (1991).
- ⁵F. J. Cadeu, T. D. Cheung, and L. Wickramasekara, J. Magn. Magn. Mater. **54–57**, 535 (1986).
- ⁶K. D. Aylesworth, Z. R. Zhao, D. J. Sellmyer, and G. C. Hadjipanayis, J. Appl. Phys. **64**, 5742 (1988).
- ⁷J. F. Zasadzinski, C. U. Segre, and E. D. Rippert, J. Appl. Phys. **61**, 4278 (1987).
- ⁸H. Homburg, Th. Sinnemann, S. Methfessel, M. Rosenberg, and B. X. Gu, J. Magn. Magn. Mater. **83**, 231 (1990).
- ⁹B. A. Kapitanov, N. V. Komilov, Ya. L. Linestsky, and V. Yu. Tsvetkov, J. Magn. Magn. Mater. **127**, 289 (1993).
- ¹⁰H. Lemke, S. Müller, T. Göddenhenrich, and C. Heiden, Phys. Status Solidi A **150**, 723 (1995).
- ¹¹S. Parhofer, G. Gieres, J. Wecker, and L. Schultz, J. Magn. Magn. Mater. **163**, 32 (1996).
- ¹²H. Sun, T. Tomida, S. Hirsosawa, and Y. Maehara, J. Magn. Magn. Mater. **164**, 18 (1996).
- ¹³D. J. Keavney, E. E. Fullerton, J. E. Pearson, and S. D. Bader, J. Appl. Phys. **81**, 4441 (1997).
- ¹⁴R. Skomski and J. M. D. Coey, Phys. Rev. B **48**, 15812 (1993).
- ¹⁵I. A. Al-Omari and D. J. Sellmyer, Phys. Rev. B **52**, 3441 (1995).
- ¹⁶J. Wecker and L. Schultz, J. Appl. Phys. **62**, 990 (1987).
- ¹⁷W. C. Stoner and E. P. Wohlfarth, Philos. Trans. R. Soc. London, Ser. A **240**, 599 (1948).
- ¹⁸G. C. Hadjipanayis and W. Gong, J. Appl. Phys. **64**, 5559 (1988).
- ¹⁹R. Fischer and H. Kronmüller, Phys. Rev. B **54**, 7284 (1996).